Implications of the Unitarity Triangle 'uc' for J, δ and $|V_{CKM}|$ elements.

Monika Randhawa[1], V. Bhatnagar[1], P.S. Gill[1,2] and M. Gupta[1]
[1] *Department of Physics, Panjab University, Chandigarh- 160 014, India.*
[2] *Sri Guru Gobind Singh College, Chandigarh-160 026, India.*

February 1, 2008

Abstract

The Jarlskog rephasing invariant parameter $|J|$ is evaluated using one of the six Unitarity Triangles involving well known CKM matrix elements $|V_{ud}|$, $|V_{us}|$, $|\frac{V_{ub}}{V_{cb}}|$, $|V_{cd}|$, $|V_{cs}|$ and $|V_{cb}|$. With PDG2000 values of $|V_{ud}|$ etc. as input, we obtain $|J| = (2.71 \pm 1.12) \times 10^{-5}$, which in the PDG representation of CKM matrix leads to the range 21^o *to* 159^o for the CP violating phase δ. The CKM matrix elements evaluated using this range of δ are in agreement with the PDG CKM matrix. The implications of refinements in the input on $|J|$, δ and CKM matrix elements have also been studied.

Recent discovery of neutrino oscillations in atmospheric neutrinos by the SuperKamiokande Collaboration [1] has not only given the first clear cut signal for physics beyond the standard model (SM), but has also triggered great amount of activity in neutrino mixing phenomena as well as in the related issue of fermion mass matrices. This has also given an impetus to study more deeply the quark mixing phenomena which have been under investigation for the last two decades. In fact, there is a need to closely examine the quark mixing phenomena in the hope that one may decipher some signal, howsoever faint, for physics beyond the SM.

In the context of quark mixing phenomena, over the last two decades, several analyses have been carried out [2], some of these in the last few years [3]. The basic purpose of these analyses has been the evaluation of Cabibbo, Kobayashi and Maskawa matrix (V_{CKM}) elements defined as,

$$\begin{pmatrix} d' \\ s' \\ b' \end{pmatrix} = \begin{pmatrix} V_{ud} & V_{us} & V_{ub} \\ V_{cd} & V_{cs} & V_{cb} \\ V_{td} & V_{ts} & V_{tb} \end{pmatrix} \begin{pmatrix} d \\ s \\ b \end{pmatrix}. \qquad (1)$$

The usual inputs for the analyses are the CP violating parameters, ϵ_K and $\epsilon_K^{'}$, as well as $B_o - \bar{B_o}$ mixing phenomenon besides unitarity of CKM matrix defined as

$$\sum_{\alpha=d,s,b} V_{i\alpha} V_{j\alpha}^* = \delta_{ij}, \tag{2}$$

$$\sum_{i=u,c,t} V_{i\alpha} V_{i\beta}^* = \delta_{\alpha\beta}. \tag{3}$$

where Latin subscripts run over the up type quarks (u, c, t) and Greek ones run over the down type quarks (d, s, b). These analyses have given considerable insight into the dynamics of CKM matrix elements and their consequences, in particular the unitarity triangle (UT) based analyses [4, 5, 6] have considerably sharpened the relationship between the CP violation and B - decays. However, it is to be noted that in these analyses, the effect of unitarity, ϵ_K and $B_o - \bar{B_o}$ mixing etc. on the CKM matrix elements is carried out simultaneously. In other words, the separate implications of unitarity, ϵ_K and $B_o - \bar{B_o}$ mixing have not been studied, in particular, on such important quantities as CP violating phase δ and CKM matrix elements involving t quark.

In view of the availability of rephasing the quark fields [2], the CKM matrix has 36 representations, therefore it has been advocated in the literature that the analysis of CKM phenomenology should be carried out in a rephasing invariant manner [4, 7, 8]. In this context Jarlkog [8] has defined an interesting quantity J which is rephasing invariant as well as all CP violating effects within the CKM paradigm are proportional to it. Interestingly J is also directly related to the commutator of the quark mass matrices [8], for example,

$$\begin{aligned} det[mm^{\dagger}, m^{'}m^{'\dagger}] &= -2iJ(m_t^2 - m_c^2)(m_c^2 - m_u^2)(m_u^2 - m_t^2) \\ &\quad \times (m_b^2 - m_s^2)(m_s^2 - m_d^2)(m_d^2 - m_b^2). \end{aligned} \tag{4}$$

Therefore an evaluation of $|J|$ based on data is going to have important implications for texture specific mass matrices in the sense that it could provide valuable clues for searching the right texture for fermion mass matrices [9].

In the very recent analyses, Parodi *et al* [10] and Mele [11] primarily concentrate on finding CKM parameters in the Wolfenstein parametrization [12] and the angles of unitarity triangle, while J. Swain *et al* [13] determine CKM parameters with and without unitarity. The PDG analysis [14, 15] evaluates the CKM matrix elements using the measured CKM elements and the unitarity as implied by the nine equations given by 2 and 3. These analyses, however, have not been carried out in the rephasing invariant manner as well as they do not evaluate J. Therefore a rephasing invariant analysis of the CKM matrix based on unitarity is very much desirable in the hope that this may sharpen the predictions of unitarity for CKM matrix elements.

The purpose of the present Rapid Communication is to evaluate $|J|$, based on non zero CP violation and on the unitarity triangle expressed by the relation,

$$V_{ud}V_{cd}^* + V_{us}V_{cs}^* + V_{ub}V_{cb}^* = 0 \tag{5}$$

and referred to as uc triangle. This is the only unitarity triangle out of the six implied by equations 2 and 3 with $i \neq j$ and $\alpha \neq \beta$, which involves well determined CKM matrix elements. After evaluating $|J|$, we use the PDG representations of V_{CKM} to find CP violating phase δ and the elements of CKM matrix involving t quark. We also intend to examine the implications of present as well as future refinements in measured V_{CKM} elements on fixing δ.

To begin with, we evaluate $|J|$, defined as [16]

$$Im[V_{\alpha j}V_{\beta k}V_{\alpha k}^*V_{\beta j}^*] = J\sum_{\gamma,l}\epsilon_{\alpha,\beta,\gamma}\epsilon_{j,k,l}. \tag{6}$$

In principle one can evaluate $|J|$ using the above formula, however, in practice it does not help much as it involves CP violating phase δ, the least known CKM parameter. Therefore, for the purpose of our analysis, we exploited the relationship of $|J|$ with the unitarity triangle. Out of the six possible unitarity triangles we have used the triangle expressed through the equation 5. As mentioned earlier this triangle involves only those CKM elements which have been directly measured, consequently $|J|$ can be evaluated through the relation,

$$|J| = 2 \times Area \;\; of \;\; the \;\; Unitarity \;\; Triangle. \tag{7}$$

With the availabilty of PDG2000 CKM elements [15], it is natural to use these as input for evaluating $|J|$, however, with a view to understand the effect of refinements in CKM matrix elements on $|J|$, we have also done our calculations with PDG98 [14] values. In the same vein we have also carried our calculations for "future" values of CKM elements which may be available in future. In table 1 we have given the PDG98 [14] values of V_{CKM} elements, $|V_{ud}|$, $|V_{us}|$, $|\frac{V_{ub}}{V_{cb}}|$, $|V_{cd}|$, $|V_{cs}|$ and $|V_{cb}|$, as well as the recent PDG2000 values and "future" values. While listing the "future" values, we have considered only those elements in which the present error is more than 15%.

Before proceeding further, it is to be noted that the triangle mentioned above is highly squashed. The sides of the triangle represented by $|V_{ud}^*V_{cd}|$ (= a) and $|V_{us}^*V_{cs}|$ (= b) are of comparable lengths while the third side $|V_{ub}^*V_{cb}|$ (= c) is several orders of magnitude smaller compared to a and b. This creates complications for evaluating the area of the triangle without violating unitarity and the existence of CP violation. To avoid these complications we have used

the constraints $|a| + |c| > |b|$ and $|b| + |c| > |a|$ as suggested by Branco and Lavoura [6]. Using these constraints and the experimental data given in the column II of table 1 (PDG98), we have generated a histogram shown in figure 1. In generating the histogram all inputs i.e. $|V_{ud}|$, $|V_{us}|$, $|\frac{V_{ub}}{V_{cb}}|$, $|V_{cd}|$, $|V_{cs}|$ and $|V_{cb}|$ have been taken at their 90% confidence level facilitating comparison with the corresponding PDG analysis. A Gaussian is fitted into the histogram plotted with approximately 30,000 entries as shown in figure 1. The resulting value of $|J|$ is given as,

$$|J| = (2.28 \pm 0.86) \times 10^{-5}, \tag{8}$$

which in the 90% C.L. leads to the range,

$$|J| = (0.87 - 3.69) \times 10^{-5}. \tag{9}$$

The value of $|J|$ can now be used to calculate δ using the PDG representations of CKM matrix, for example,

$$V_{CKM} = \begin{pmatrix} c_{12}c_{13} & s_{12}s_{13} & s_{13}e^{-i\delta} \\ -s_{12}c_{23} - c_{12}s_{23}s_{13}e^{i\delta} & c_{12}c_{23} - s_{12}s_{23}s_{13}e^{i\delta} & s_{23}c_{13} \\ s_{12}s_{23} - c_{12}c_{23}s_{13}e^{i\delta} & -c_{12}s_{23} - s_{12}c_{23}s_{13}e^{i\delta} & c_{23}c_{13} \end{pmatrix}, \tag{10}$$

with $c_{ij} = cos\theta_{ij}$ and $s_{ij} = sin\theta_{ij}$ for the generation labels $i, j = 1, 2, 3$. In the above representation, J can be expressed as,

$$J = J^{'} sin\delta, \tag{11}$$

where,

$$J^{'} = sin\theta_{12} sin\theta_{23} sin\theta_{13} cos\theta_{12} cos\theta_{23} cos^2\theta_{13}. \tag{12}$$

Before evaluating $J^{'}$, using equation 1 we calculate $sin\theta_{12}$, $sin\theta_{23}$ and $sin\theta_{13}$ from the experimental values of $|V_{us}|$, $|\frac{V_{ub}}{V_{cb}}|$, and $|V_{cb}|$ given in table 1. The corresponding values of $sin\theta_{12}, sin\theta_{23}$ $sin\theta_{13}$, presented in table 2, are used to evaluate $J^{'}$. Following the procedure outlined above for evaluating $|J|$, with all input values at their 90% C.L., $J^{'}$ comes out to be,

$$J^{'} = (2.86 \pm 0.76) \times 10^{-5}. \tag{13}$$

The range corresponding to 90% C.L. of $J^{'}$ can be easily found out and is given as,

$$J^{'} = (1.61 - 4.11) \times 10^{-5}. \tag{14}$$

Using equation 11, we can find the range of δ corresponding to various C.Ls. of $|J|$ and $J^{'}$. In this regard in figure 2, we have plotted $J^{'} sin\delta$ as a function of δ. The upper and lower sinusoidal curves correspond to upper and lower

limits of $J^{'}$ given by equation 13. The horizontal lines depict upper and lower limits of $|J|$ given by equation 8. Since $J^{'} sin\delta$ should reproduce $|J|$ calculated through the unitarity triangle uc, therefore from figure 2, by comparing the two one can easily find out the widest limits on δ, for example,

$$\delta = 23^o \; to \; 157^o. \tag{15}$$

The above range of δ corresponds to 1σ C.L. of both $|J|$ and $J^{'}$. Similarly, using 9 and 14, the corresponding range of δ at 90% C.L. of $|J|$ and $J^{'}$ can be found out as shown in figure 3 and is given as,

$$\delta = 12^o \; to \; 168^o. \tag{16}$$

These values of δ apparently look to be the consequence only of the unitarity relationship given by equation 5. However on further investigation, as shown by Branco and Lavoura [6], one finds that these δ ranges are consequences of all the non trivial unitarity constraints. In this sense the above range could be attributed to as a consequence of unitarity of the CKM matrix.

Alternatively, using equation 11, one can find out δ for each of the 30,000 entries and likewise plot a histogram for δ. Again fitting a Gaussian to the histogram, δ comes out to be,

$$\begin{aligned} \delta &= 51^o \pm 21^o \; (I \; quadrant), \\ & \quad 129^o \pm 21^o \; (II \; quadrant). \end{aligned} \tag{17}$$

The corresponding range of δ at 90% C.L. is,

$$\begin{aligned} \delta &= 17^o \; to \; 85^o \; (I \; quadrant), \\ & \quad 95^o \; to \; 163^o \; (II \; quadrant). \end{aligned} \tag{18}$$

This gives us relatively stronger bounds on δ. However, for the subsequent calculations we have used ranges of δ as given by 15 and 16.

As has been mentioned earlier, we intend to compare our results both with PDG98 [14] as well as with PDG2000 [15] CKM matrix. To begin with, as the input for $|J|$ has been from PDG98 values, therefore we compare our results with PDG98 CKM matrix. To calculate the CKM elements, we have used the values of sines of mixing angles at their 90% C.L. (using column II of table 2) and δ at 90% C.L. of $|J|$ (equation 16). The calculated V_{CKM} matrix is,

$$\left[\begin{array}{ccc} 0.9747 - 0.9765 & 0.216 - 0.223 & 0.0019 - 0.0045 \\ 0.216 - 0.223 & 0.9739 - 0.9757 & 0.037 - 0.042 \\ 0.004 - 0.014 & 0.035 - 0.042 & 0.9992 \end{array} \right]. \tag{19}$$

To facilitate the comparison of corresponding CKM matrix elements as well as for easy readability, we present below the V_{CKM} from the PDG98 [14] also calculated at 90% C.L..

$$\begin{bmatrix} 0.9745-0.9760 & 0.217-0.224 & 0.0018-0.0045 \\ 0.217-0.224 & 0.9737-0.9753 & 0.036-0.042 \\ 0.004-0.013 & 0.035-0.042 & 0.9991-0.9994 \end{bmatrix}. \quad (20)$$

Comparing 19 and 20, one finds that we have been able to reproduce PDG matrix with minor differences only at fourth decimal places. In addition to the reproduction of CKM matrix elements, it needs to be emphasized that we have calculated $|J|$ and δ based entirely on unitarity and data, which to our knowledge has not been calculated earlier. The availabilty of $|J|$ and δ simplifies the task of calculating CKM matrix elements as well as giving a deeper insight into the contribution of CKM paradigm to CP violating phenomena.

The above method of evaluating $|J|$, δ and CKM matrix elements can be easily repeated for the PDG2000 as well as "future" values of input parameters mentioned in tables 1 and 2. The corresponding $|J|$ and δ have been given in table 3. For the sake of completeness, we have repeated the whole analysis with input values at their 1σ and 3σ C.Ls. and the corresponding results for $|J|$, $J^{'}$ and δ are listed in table 3.

A close look at the table 3 leads us to several interesting points. For example, the bounds on $|J|$ and δ are weak when the input values are taken at their 3σ C.L., but we get relatively stronger bounds when the analysis is done with the input values being at their 90% and 1σ C.L.. Further, it is clear from the same table that there is not much change in the range of δ with PDG98 and PDG2000 values. However, if in future the ranges of $|V_{cs}|$ and $|\frac{V_{ub}}{V_{cb}}|$ are further constrained, lt may lead to significant narrowing in the range of δ so obtained, as shown in columns V and VI of row IV of table 3.

To give a better insight into the implications of PDG2000 values on our calculations, we present below the CKM matrix evaluated using values of sines of mixing angles at their 90% C.L. (from column III of table 2) and δ at 90% C.L. of $|J|$.

The calculated V_{CKM} matrix is,

$$\begin{bmatrix} 0.9756-0.9765 & 0.216-0.223 & 0.002-0.005 \\ 0.216-0.223 & 0.9739-0.9757 & 0.037-0.043 \\ 0.005-0.013 & 0.036-0.043 & 0.9992 \end{bmatrix}. \quad (21)$$

To facilitate the comparison, we present below the V_{CKM} from the PDG2000 [15] also calculated at 90% C.L..

$$\begin{bmatrix} 0.9742-0.9757 & 0.219-0.226 & 0.002-0.005 \\ 0.219-0.225 & 0.9734-0.9749 & 0.037-0.043 \\ 0.004-0.014 & 0.035-0.043 & 0.9990-0.9993 \end{bmatrix}. \quad (22)$$

Comparing the CKM matrices 21 and 22, we see that we are able to reproduce PDG2000 CKM matrix, once again justifying the procedure followed in carrying out the present analysis. To assess the impact of future refinements in CKM matrix elements $|\frac{V_{ub}}{V_{cb}}|$ and $|V_{cs}|$, we present below the CKM matrix elements corresponding to $|J|$ and δ as mentioned in row III of table 3.

$$\begin{bmatrix} 0.9747 - 0.9765 & 0.216 - 0.223 & 0.0029 - 0.0043 \\ 0.216 - 0.223 & 0.9739 - 0.9757 & 0.037 - 0.043 \\ 0.006 - 0.013 & 0.036 - 0.043 & 0.9992 \end{bmatrix}. \qquad (23)$$

Comparing 19, 21 and 23 we find that the $|V_{CKM}|$ matrix elements do not show much variation when the latest [15] or the "future" values are used. The small changes in the CKM elements mostly at the fourth decimal places are not primarily due to change in the range of δ, but due to overall changes in all the input parameters. This probably restricts the use of unitarity in evaluating the $|V_{CKM}|$ elements involving t quark.

In conclusion, we would like to mention that using only one of the six unitarity triangles, we have evaluated Jarlskog rephasing invariant parameter $|J|$ and consequently δ. Using this range of δ we have been able to reproduce the PDG matrix at 90% C.L. evaluated by PDG group. Our calculations also indicate that improvements and further refinements in V_{CKM} elements $|V_{cs}|$ and $|\frac{V_{ub}}{V_{cb}}|$ result in significant narrowing in the range of δ, however there is no appreciable impact on V_{CKM} elements involving t quark, therefore, their range can be narrowed only by direct measurement of δ. It needs to be mentioned that an evaluation of $|J|$ based on data is going to have important implications for texture specific mass matrices as the parameter J is directly related to the mass matrices. Our conclusions in this regard would be published elsewhere.

ACKNOWLEDGMENTS

M.R. would like to thank CSIR, Govt. of India, for financial support. M.R. and P.S.G. would like to thank the chairman, Department of Physics, for providing facilities to work in the department. P.S.G. acknowledges the financial support received for his UGC project.

References

[1] Superkamiokande collaboration; Y. Fukuda et. al., Phys. Lett. **B433**, 9(1998) and **B436**, 33(1998);
T Kajita, Talk presented at Neutrino-98, Takayama, Japan (1998).

[2] CP violation, Ed. L. wolfenstein, North Holland, elsevier Science Publishers B.V., 1989; CP violation, Ed. C. Jarlskog, World Scientific Publishing Co. Pte. Ltd, 1989; G. Buchalla, Andrzej J. Buras, M. E. Lautenbacher, Rev. Mod. Phys. **68**, 1125(1996) and references therein;

[3] Manmohan Gupta and P. S. Gill, Pramana **38**, 477(1992); Stefan Herrlich and Ulrich Nierste, Phys. Rev. **D52**, 6505(1995); M. Gronau and J. L. Rosner, Phys. Rev. Lett. **76**, 1200(1996); A. Buras, in "Probing the Standard Model of Particle Interactions", F. David and R. Gupta, Eds, 1998 Elsevier Science B. V.; P. S. Gill and Manmohan Gupta, Mod. Phys. Lett. **A13**, 2445(1998). H. Fritzsch and Z. Z. Xing, Nucl. Phys. **B556**, 49(1999); A. Ali, in Proc. of the 13th Topical Conference on Hadron Collider Physics, TIFR, Mumbai, India (1999); I. I. Bigi and A. I. Sanda, hep-ph/9909479.

[4] A. Campa, C. Hamzaoui and V. Rahal, Phys. Rev. **D39**, 3435(1989).

[5] Stefan Herrlich and Ulrich Nierste, Phys. Rev. **D52**, 6505(1995); M. Gronau and J. L. Rosner, Phys. Rev. Lett. **76**, 1200(1996); H. Fritzsch and Z. Z. Xing, Nucl. Phys. **B556**, 49(1999); A. Ali, in Proc. of the 13th Topical Conference on Hadron Collider Physics, TIFR, Mumbai, India (1999); I. I. Bigi and A. I. Sanda, hep-ph/9909479.

[6] G.C. Branco and L. Lavoura, Phys. Lett. **B208**, 123(1988).

[7] Y. Koide et al., Univ Shizuoka, US91-04(1991); G. Belanger, E. Boridy, C. Hamzaoui and G. G. Jakimov, Phys. Rev. **D48**, 4275(1993).

[8] C. Jarlskog, Phys. Rev. Lett. **55**, 1039(1985); Zeit f. Phys. **C29**, 491(1985).

[9] A. Campa, C. Hamzaoui and V. Rahal, Phys. Rev. **D39**, 3435(1989); P. S. Gill and Manmohan Gupta, J. Phys **G23**, 335(1997); Phys. Rev. **D56** 3143(1997); H. Fritzsch and Z. Z. Xing, Nuc. Phys. **B556**, 49(1999).

[10] F. Parodi, P. Roudeau and A. Stocchi, Nuovo Cim. **A112**, 833(1999).

[11] S. Mele, hep-ph/9808411, Proceedings of workshop on CP violation, Adelaide, Australia, July 3-8(1998).

[12] L. Wolfenstein, Phys. Rev. Lett. **51**, 1945(1983).

[13] John Swain and Lucas Taylor, hep-ph/9712421.

[14] C. Caso et. al., Particle Data Group, Euro. Phys. J. **C3**, 1(1998).

[15] D.E. Groom et. al., Particle Data group, Euro. Phys. J. **C15**, 1(2000).

[16] C. Jarlskog, Proc. of 1986 Rencontre de moriond on "Progress in electroweak interactions", (Ed. J. Tran Thanh Vass) p. 389.

Element	PDG98 values	PDG2000 values	"Future" values
$\|V_{ud}\|$	0.9740 ± 0.0010	0.9735 ± 0.0008	0.9735 ± 0.0008
$\|V_{us}\|$	0.2196 ± 0.0023	0.2196 ± 0.0023	0.2196 ± 0.0023
$\|\frac{V_{ub}}{V_{cb}}\|$	0.08 ± 0.02	0.090 ± 0.025	0.090 ± 0.010
$\|V_{cd}\|$	0.224 ± 0.016	0.224 ± 0.016	0.224 ± 0.016
$\|V_{cs}\|$	1.04 ± 0.16	1.04 ± 0.16	1.04 ± 0.08
$\|V_{cb}\|$	0.0395 ± 0.0017	0.0402 ± 0.0019	0.0402 ± 0.0019

Table 1: The experimental values of V_{CKM} elements, $|V_{ud}|$, $|V_{us}|$, $|\frac{V_{ub}}{V_{cb}}|$, $|V_{cd}|$, $|V_{cs}|$ and $|V_{cb}|$.

Parameter	Input PDG98 values	Input PDG2000 values	Input "Future" values
$sin\theta_{12}$	0.2196 ± 0.0023	0.2196 ± 0.0023	0.2196 ± 0.0023
$sin\theta_{23}$	0.0395 ± 0.0017	0.0402 ± 0.0019	0.0402 ± 0.0019
$sin\theta_{13}$	0.0032 ± 0.0008	0.0036 ± 0.0010	0.0036 ± 0.0004

Table 2: Sines of the mixing angles calculated from the data given in table 1.

		$\|J\|$	$J^{'}$	δ obtained graphically with $\|J\|$ and $J^{'}$ at 1σ C.L.	δ obtained graphically with $\|J\|$ and $J^{'}$ at 90% C.L.
PDG98	All inputs at 1σ C.L.	$(2.21 \pm .62) \times 10^{-5}$	$(2.76 \pm .44) \times 10^{-5}$	$30^o - 150^o$	$20^o - 160^o$
	All inputs at 90% C.L.	$(2.28 \pm .86) \times 10^{-5}$	$(2.86 \pm .76) \times 10^{-5}$	$23^o - 157^o$	$12^o - 168^o$
	All inputs at 3σ C.L.	$(2.65 \pm 1.37) \times 10^{-5}$	$(3.26 \pm 1.30) \times 10^{-5}$	$16^o - 164^o$	$4^o - 176^o$
PDG2000	All inputs at 1σ C.L.	$(2.59 \pm .79) \times 10^{-5}$	$(3.23 \pm 0.63) \times 10^{-5}$	$28^o - 152^o$	$18^o - 162^o$
	All inputs at 90% C.L.	$(2.71 \pm 1.12) \times 10^{-5}$	$(3.41 \pm 1.06) \times 10^{-5}$	$21^o - 159^o$	$10^o - 170^o$
	All inputs at 3σ C.L.	$(3.29 \pm 1.78) \times 10^{-5}$	$(4.14 \pm 1.67) \times 10^{-5}$	$15^o - 165^o$	$3^o - 177^o$
"Future" values	All inputs at 1σ C.L.	$(2.79 \pm 0.49) \times 10^{-5}$	$(3.14 \pm 0.31) \times 10^{-5}$	$42^o - 138^o$	$32^o - 148^o$
	All inputs at 90% C.L.	$(2.61 \pm 0.78) \times 10^{-5}$	$(3.19 \pm 0.49) \times 10^{-5}$	$30^o - 150^o$	$19^o - 161^o$
	All inputs at 3σ C.L.	$(2.73 \pm 1.09) \times 10^{-5}$	$(3.34 \pm 0.89) \times 10^{-5}$	$23^o - 157^o$	$11^o - 169^o$

Table 3: $|J|$, $J^{'}$ and δ values obtained by using PDG98, PDG2000 and "future values" of input parameters listed in table 1 and 2 at their 1σ, 90% and 3σ C.L.'s

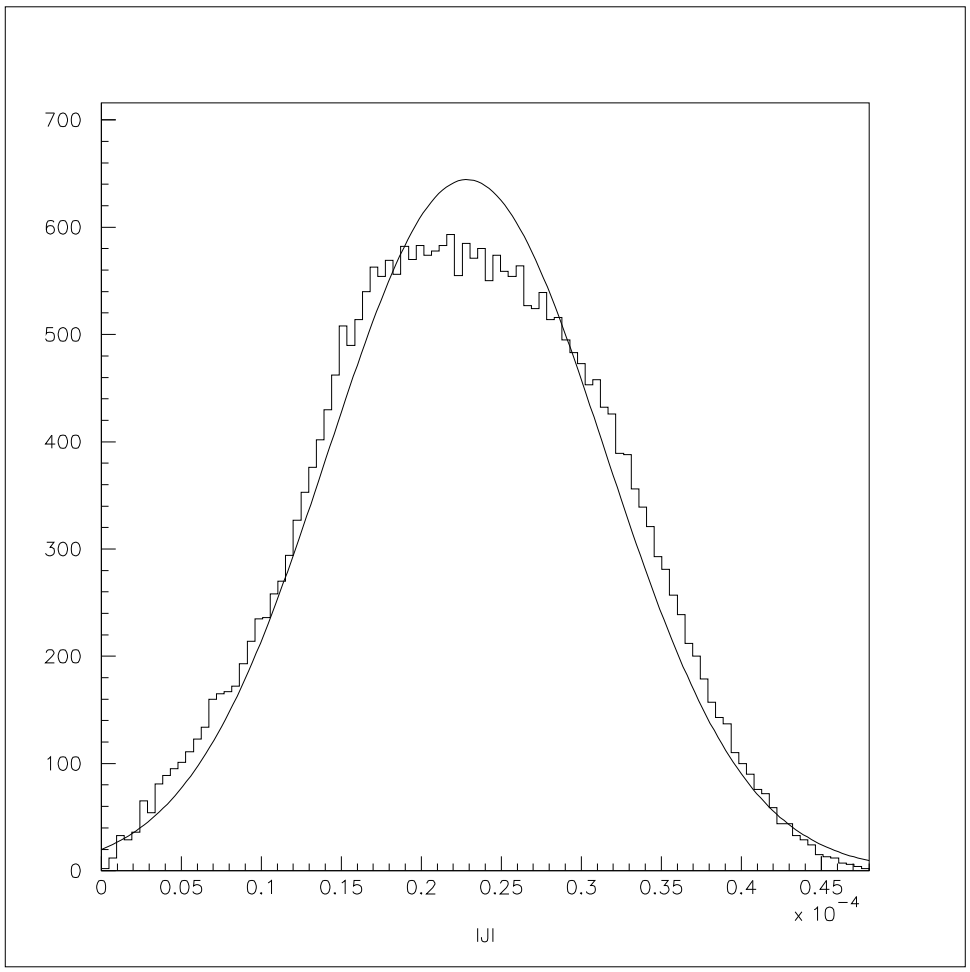

Figure 1: The histogram as well as the gaussian fit of $|J|$ generated by considering input parameters at their 90% confidence level.

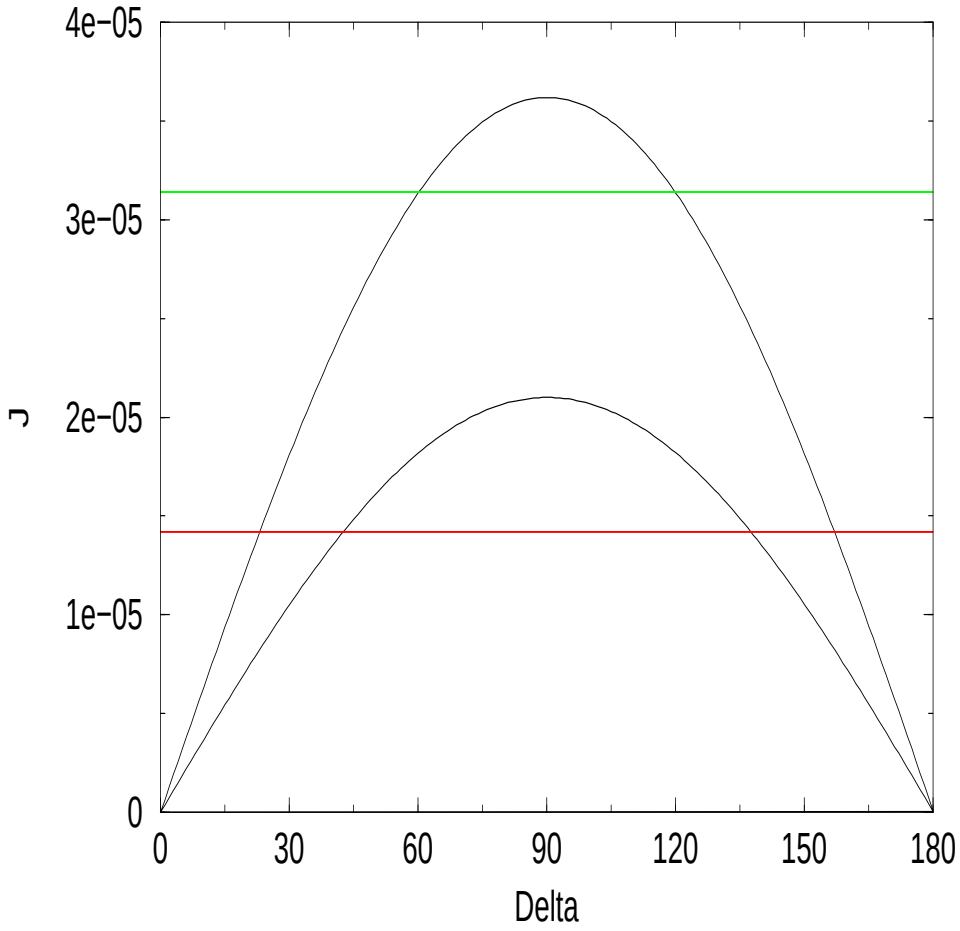

Figure 2: Plot of $J(= J^{'} sin\delta)$ vs. δ. The upper and lower sinusoidal curves correspond to upper and lower limits of $J^{'}$ given by equation 13. The horizontal lines depict upper and lower limits of $|J|$ given by equation 8.

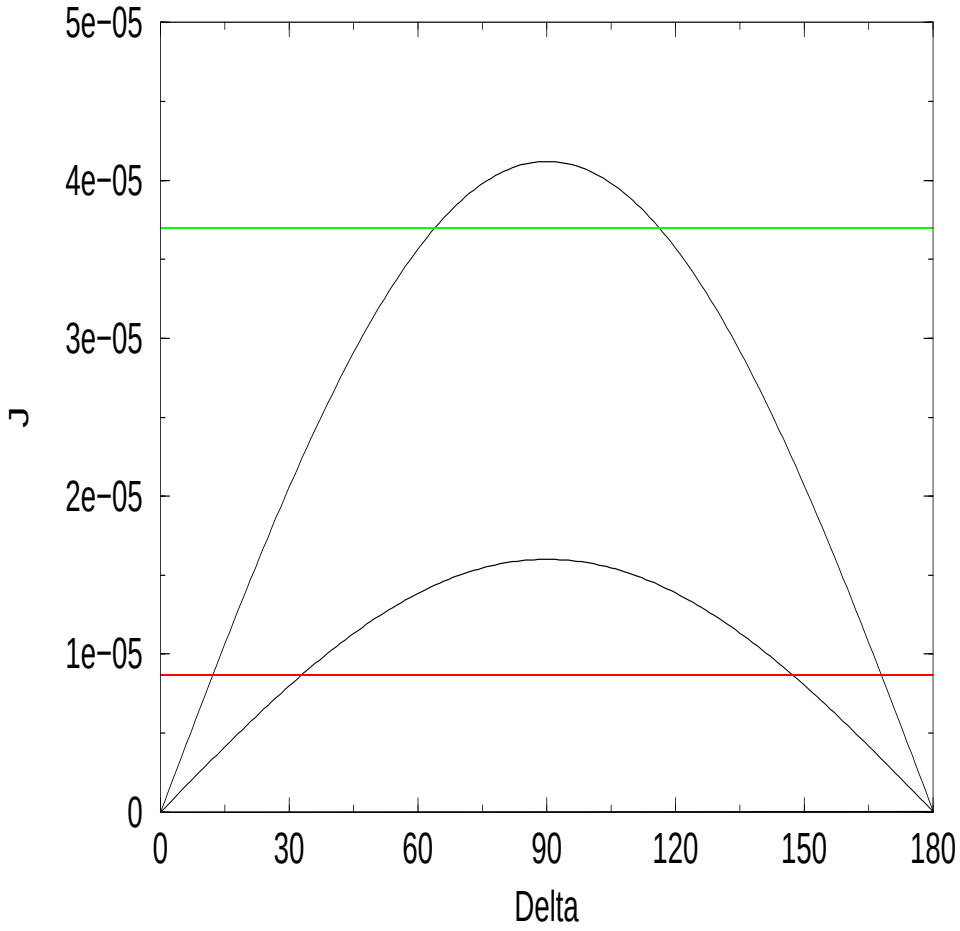

Figure 3: Plot of $J(= J^{'} sin\delta)$ vs. δ. The upper and lower sinusoidal curves correspond to upper and lower limits of $J^{'}$ given by equation 14. The horizontal lines depict upper and lower limits of $|J|$ given by equation 9.